

Numerical study of magnetization processes in rare-earth tetraborides

Pavol Farkašovský, Hana Čenčariková, and Slavomír Mat’áš

Institute of Experimental Physics, Slovak Academy of Sciences, Watsonova 47, 040 01 Košice, Slovakia

(Received 13 April 2010; revised manuscript received 18 May 2010; published 6 August 2010)

We present a simple model for a description of magnetization processes in rare-earth tetraborides. The model is based on the coexistence of two subsystems, and, namely, the spin subsystem described by the Ising model and the electronic subsystem described by the Falicov-Kimball model on the Shastry-Sutherland lattice (SSL). Moreover, both subsystems are coupled by the anisotropic spin-dependent interaction of the Ising type. We have found, that the switching on of the spin-dependent interaction (J_z) between the electron and spin subsystems and taking into account the electron hopping on the nearest (t) and next-nearest (t') lattice sites of the SSL leads to a stabilization of magnetization plateaus. In addition, to the Ising magnetization plateau at $m^{sp}/m_s^{sp}=1/3$ we have found three relevant magnetization plateaus located at $m^{sp}/m_s^{sp}=1/2$, $1/5$, and $1/7$ of the saturated spin magnetization m_s^{sp} . The ground states corresponding to magnetization plateaus have the same spin structure consisting of parallel antiferromagnetic bands separated by ferromagnetic stripes.

DOI: 10.1103/PhysRevB.82.054409

PACS number(s): 75.10.-b, 75.60.Ej, 75.40.Mg

I. INTRODUCTION

The Shastry-Sutherland lattice (SSL) was considered more than 20 years ago by Shastry and Sutherland¹ as an interesting example of a frustrated quantum spin system with an exact ground state. It can be described as a square lattice with antiferromagnetic couplings J between nearest neighbors and additional antiferromagnetic couplings J' between next-nearest neighbors in every second square (see Fig. 1). This lattice attracted much attention after its experimental realization in the $\text{SrCu}_2(\text{BO}_3)_2$ compound.² The observation of a fascinating sequence of magnetization ($m/m_s=1/2$, $1/3$, $1/4$, and $1/8$ of the saturated magnetization m_s) in this material² stimulated further theoretical and experimental studies of the SSL.^{3,4}

As another realization of the SSL the rare-earth tetraborid TmB_4 has recently been studied in finite magnetic fields.⁵ Since fully polarized state can be reached for experimentally accessible magnetic fields, this compound allows exploration of its complete magnetization process. It was found that the magnetization diagram of TmB_4 consists of magnetization plateaus located at small fractional values of $m/m_s=1/7, 1/8, 1/9, \dots$ of the saturated magnetization followed by the major magnetization plateau located at $m/m_s=1/2$. Note that, due to large total magnetic moments of the magnetic ions, this compound can be considered as a classical system. Moreover, because of strong crystal field effects, the effective spin model for TmB_4 has been suggested to be described by the spin-1/2 Shastry-Sutherland model under strong Ising (or easy-axis) anisotropy.⁵ From this point of view it was natural to begin a description of magnetization process in the TmB_4 material from the Ising limit on the SSL that can be, in the presence of a finite magnetic field h , expressed as follows:

$$H_{JJ'} = J \sum_{\langle i,j \rangle} S_i^z S_j^z + J' \sum_{\langle\langle i,j \rangle\rangle} S_i^z S_j^z - h \sum_i S_i^z, \quad (1)$$

where $S_i^z = \pm 1/2$ denotes the z component of a spin-1/2 degree of freedom on site i of a square lattice and J, J' are the antiferromagnetic exchange couplings between all nearest-

neighbor bonds (J) and next-nearest-neighbor bonds in every second square (J'), as indicated in Fig. 1.

In spite the relative simplicity of the model Hamiltonian (1), fully different conclusions have been obtained for the magnetization curve of this model within various approaches. For example, the authors of Ref. 5 found, analyzing a finite system consisting of 16 spins, a single magnetization plateau at $1/2$ of the saturated magnetization in accordance with experimental data in TmB_4 . However, numerical simulations obtained within the Monte Carlo and tensor renormalization-group methods on much larger systems^{6,7} did not confirm this conclusion. In contrast to previous results they showed that the Ising model on the SSL exhibits in the presence of the magnetic field the magnetization plateau only at $1/3$ of the saturated magnetization. Thus the different conclusion of Ref. 5 appears to be due to the usage of inappropriate finite lattice sizes.

The existence of the magnetization plateau at only $1/3$ of the saturated magnetization and its absence at $1/2$ indicates that it is necessary to go beyond the classical Ising limit to reach the correct description of the magnetization process in TmB_4 and other rare-earth tetraborides. An attempt has been

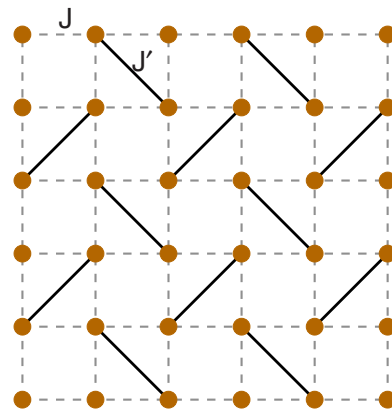


FIG. 1. (Color online) The Shastry-Sutherland lattice with magnetic couplings J bonds along the edges of the squares and J' along the diagonals.

done by Meng and Wessel⁶ who studied the spin-1/2 easy-axis Heisenberg model on the SSL with ferromagnetic transverse spin exchange using quantum Monte Carlo and degenerate perturbation theory. Besides the magnetization plateau at 1/3 of the saturated magnetization they found a further plateau at 1/2, which persists only in the quantum regime. The same results have been obtained by Liu and Sachdev analyzing the perturbative effects of the transverse fluctuations on the SSL spin multiplets with large easy-axis anisotropy.⁸

It should be noted that a similar behavior as for TmB₄ has been also observed for other rare-earth tetraborides. For example, for ErB₄ the magnetization plateau has been found at $m/m_s=1/2$,^{9,10} for TbB₄ at $m/m_s=1/2, 4/9, 1/3, 2/9$, and $7/9$,¹¹ and for HoB₄ at $m/m_s=1/3, 4/9$, and $3/5$.¹⁰

II. MODEL

In the current paper we present an alternative model of stabilization the magnetization plateaus in the rare-earth tetraborides based on the fact that these materials, in contrast to SrCu₂(BO₃)₂, are metallic. Thus for a correct description of ground-state properties of rare-earth tetraborides one should take into account both spin and electron subsystems as well as the coupling between them. Supposing that electron and spin subsystems interact only via the spin-dependent Ising interaction J_z , the Hamiltonian of the system can be written as

$$H = \sum_{ij\sigma} t_{ij} d_{i\sigma}^\dagger d_{j\sigma} + J_z \sum_i (n_{i\uparrow} - n_{i\downarrow}) S_i^z - h \sum_i (n_{i\uparrow} - n_{i\downarrow}) + H_{JJ'}, \quad (2)$$

where $d_{i\sigma}^\dagger, d_{i\sigma}$ are the creation and annihilation operators of the itinerant electrons in the d -band Wannier state at site i and $n_{i\sigma} = d_{i\sigma}^\dagger d_{i\sigma}$. The first term of Eq. (2) is the kinetic energy corresponding to quantum-mechanical hopping of the itinerant d electrons between sites i and j . These intersite hopping transitions are described by the matrix elements t_{ij} , which are $-t$ if i and j are the nearest neighbors, $-t'$ if i and j are the next-nearest neighbors from the SSL and zero otherwise. The second term represents the above-mentioned anisotropic, spin-dependent local interaction of the Ising type between the localized spins and itinerant electrons. The third term describes an action of the magnetic field on the itinerant electrons.

The model described by Eq. (2) is a straightforward extension of the spin-one-half Falicov-Kimball model with anisotropic spin-dependent interaction introduced in Ref. 12 and discussed in detail in Refs. 13 and 14. The only differences are that we consider here a direct spin interaction (of the Ising type) between the localized spins and that the underlying lattice is of the Shastry-Sutherland type. The relation of this model to similar models of interacting electron and spin systems is extensively discussed in Ref. 14.

To examine the magnetization curve corresponding to the model Hamiltonian (2), we have used the well-controlled numerical method that we have elaborated recently to study the ground states of the spinless/spin-one-half

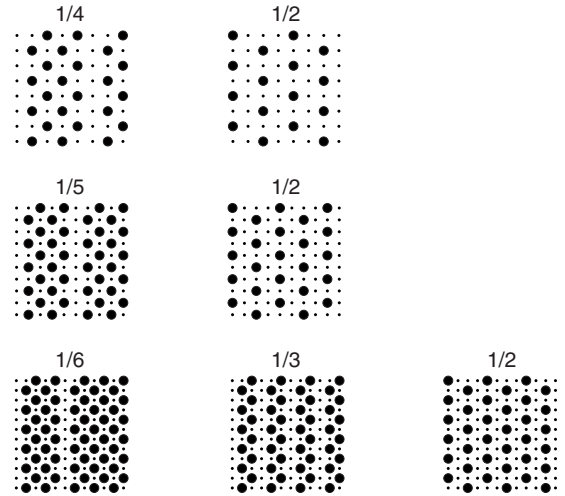


FIG. 2. The complete list of the ground-state spin configurations (for $0 < m^{sp}/m_s^{sp} < 1$) that are stable on finite intervals of h for $L=8 \times 8$, $L=10 \times 10$, and $L=12 \times 12$. The big (small) dots correspond to the up (down) spin orientation.

Falicov-Kimball model.¹³ This method is described in detail in our previous papers^{15,16} and thus we summarize here only the main steps of the algorithm: (i) chose a trial spin configuration $s = \{S_1^z, S_2^z, \dots, S_L^z\}$. (ii) Having s, J_z, t , and t' fixed, find all eigenvalues λ_k^σ of $h_\sigma(s) = t_{ij} - \sigma J_z s_i \delta_{ij}$. (iii) For a given $N = N_\uparrow + N_\downarrow$ (where N is the total number of electrons) determine the ground-state energy $E(s) = \sum_\sigma \sum_{k=1}^{N_\sigma} \lambda_k^\sigma - h(N_\uparrow - N_\downarrow) + H_{JJ'}$ of a particular spin configuration s by filling in the lowest N_\uparrow, N_\downarrow one-electron levels λ_k^σ . (iv) Generate a new configuration s' by flipping a randomly chosen spin. (v) Calculate the ground-state energy $E(s')$. If $E(s') < E(s)$ the new configuration is accepted, otherwise s' is rejected. Then the steps (ii)–(v) are repeated until the convergence (for given parameters of the model) is reached.

III. RESULTS AND DISCUSSION

Using the method discussed above we have performed exhaustive numerical studies of the model, Eq. (2), for a wide range of model parameters h, J_z, t, t' and $J/J'=1$ selected on the base of experimental measurements.⁵ To exclude the finite-size effects the numerical calculations have been done for several different Shastry-Sutherland clusters consisting of $L=8 \times 8, 10 \times 10$, and 12×12 sites. The most important result obtained from these calculations is that the switching on of J_z and t leads to a stabilization of the uniform ground-state spin arrangement consisting of parallel antiferromagnetic bands separated by ferromagnetic stripes. The stability of these striped phases has been examined for the following set of J_z, t , and t' values ($J_z=1, 2, 4; t=1, 4; t'/t=0, 0.2, 0.4, 0.6, 0.8, 1$) and it was found that this type of spin ordering persists in all cases. The complete list of the ground-state spin arrangements (for $0 < m^{sp}/m_s^{sp} < 1$) that are stable on finite intervals of magnetic field values are depicted on Fig. 2. The second important observation is that the width w of the antiferromagnetic bands cannot be arbitrary but ful-

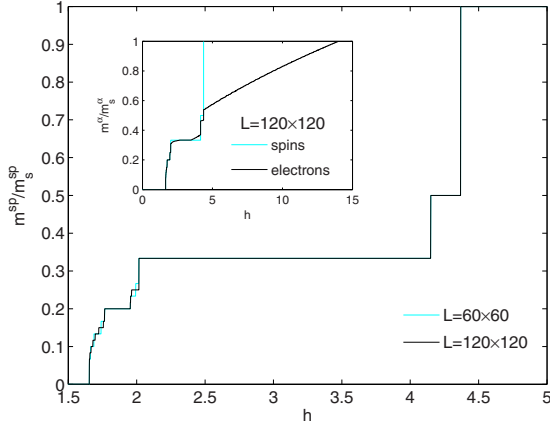


FIG. 3. (Color online) Magnetization curves for $J'/J=1$, $J_z=2$, $t=4$, $t'=0$ and different values of L . Inset: magnetization curves of spin and electron subsystems ($\alpha=el$ or sp).

fill severe restrictions. Indeed, we have found that with exception the case $m^{sp}/m_s^{sp}=1/2$, in all remaining cases the permitted width of the antiferromagnetic band is only w or $w+2$, where w is the even number. This fact is very important from the numerical point of view since it allows us to perform the numerical calculations on much larger clusters with the extrapolated set of configurations of the above described type. The resulting magnetization curves obtained on the extrapolated set of ground-state spin configurations consisting of parallel antiferromagnetic bands of width w (w and $w+2$) separated by ferromagnetic stripes are shown in Figs. 3–5 for selected values of model parameters that represent the typical behavior of the model.

One can see that the switching on of the spin-dependent interaction J_z and taking into account the electron hopping t on the nearest lattice sites of the SSL leads to a stabilization of magnetization plateaus (the next-nearest hopping integrals t' only renormalize the width of the magnetization plateaus). In addition to the Ising magnetization plateau at $m^{sp}/m_s^{sp}=1/3$ we have found two magnetization plateaus located at $m^{sp}/m_s^{sp}=1/2$ and $m^{sp}/m_s^{sp}=1/5$. The ground-state spin arrangements corresponding to these magnetization

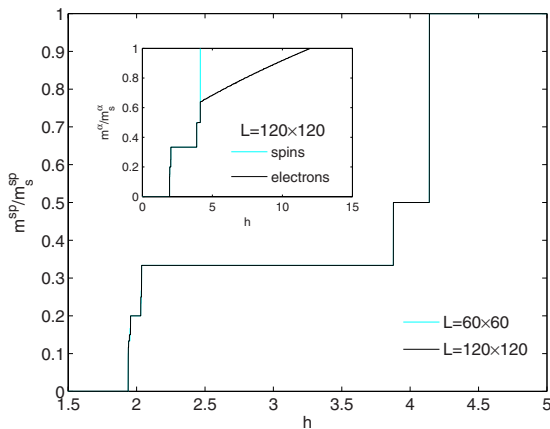


FIG. 4. (Color online) Magnetization curves for $J'/J=1$, $J_z=4$, $t=4$, $t'=0$ and different values of L . Inset: magnetization curves of spin and electron subsystems.

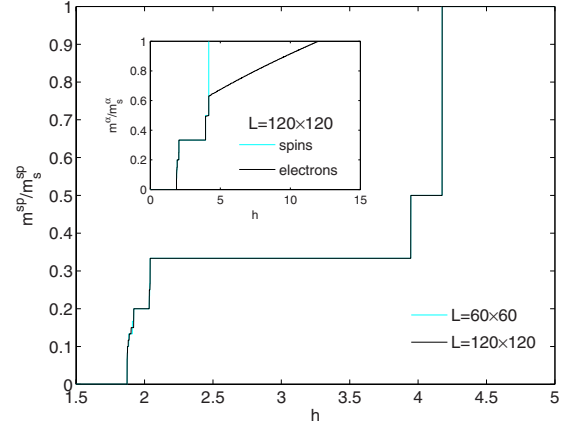


FIG. 5. (Color online) Magnetization curves for $J'/J=1$, $J_z=4$, $t=4$, $t'=0.4t$ and different values of L . Inset: magnetization curves of spin and electron subsystems.

plateaus have the same structure consisting of parallel antiferromagnetic bands of a width w (where $w=1$ for $m^{sp}/m_s^{sp}=1/2$, $w=2$ for $m^{sp}/m_s^{sp}=1/3$, and $w=4$ for $m^{sp}/m_s^{sp}=1/5$) separated by ferromagnetic stripes. Thus, our numerical results show that besides the pure spin mechanism [e.g., the easy-axis Heisenberg model on the SSL (Ref. 6)] of stabilization the magnetization plateaus in rare-earth tetraborides, there exists also an alternative mechanism based on the coexistence of electron and spin subsystems that are present in these materials. From this point of view it is interesting to compare in detail the ground states obtained within these two different approaches. For $m^{sp}/m_s^{sp}=1/3$ our results are identical with ones obtained within the Ising^{5,7} as well as easy-axis Heisenberg^{6,8} model on the SSL. The accordance between our and the easy-axis Heisenberg solution⁶ is found surprisingly also for $m^{sp}/m_s^{sp}=1/2$. In this case both approaches predict the sequence of parallel antiferromagnetic and ferromagnetic stripes. For $m^{sp}/m_s^{sp}=1/5$ our results postulate a band type of spin ordering.

While the magnetization plateaus at $m^{sp}/m_s^{sp}=1/2$ and $1/3$ have been really found in the rare-earth tetraborides,^{5,9–11} the $1/5$ -magnetization plateau in these compounds absent. Instead the $1/5$ -magnetization plateau there have been observed magnetization plateaus at smaller values of m^{sp}/m_s^{sp} , and, namely, at $m^{sp}/m_s^{sp}=1/7$, $1/9$, and $1/11$ [TmB₄ (Ref. 5)]. Since the linear sizes of selected clusters (60×60 and 120×120) are not dividable by 7, 9, and 11 the absence of magnetization plateaus at $1/7$, $1/9$, and $1/11$ is nothing surprising. To identify the magnetization plateaus at $m^{sp}/m_s^{sp}=1/7$, $1/9$, and $1/11$ one has to examine much larger lattices. For example, for the simultaneous detection of the magnetization plateaus at $m^{sp}/m_s^{sp}=1/7$, $1/9$, and $1/11$ and $m^{sp}/m_s^{sp}=1/2$, $1/3$, and $1/5$ (the stable plateaus on the 60×60 and 120×120 clusters) one should consider the cluster of linear size $L_s=2 \times 5 \times 7 \times 9 \times 11=6930$, what is far away beyond the reach of the present day computers. Thus the only way how to verify the possibility of existence the $1/7$, $1/9$, and $1/11$ plateaus is to consider smaller clusters that do not contain simultaneously all above-mentioned plateaus but only some of them. The accessible clusters for such a study are: the 70×70 and 140×140 clusters for the $1/7$

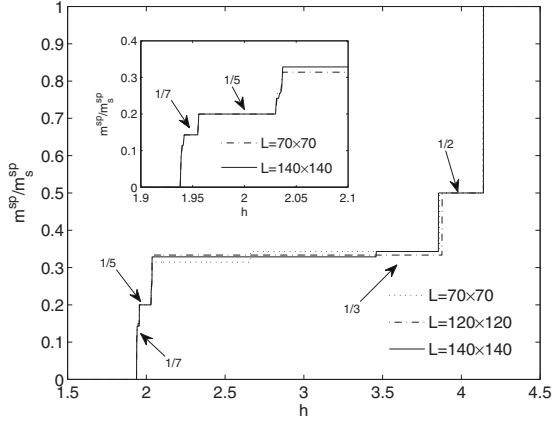


FIG. 6. Magnetization curves for $J'/J=1$, $t=4$, $t'=0$, $J_z=4$ and different values of L . Inset: a detail of magnetization curves for small h .

plateau, the 90×90 cluster for the $1/9$ plateau, and the 110×110 cluster for the $1/11$ plateau. In Fig. 6 we present magnetization curves obtained on clusters consisting of 70×70 and 140×140 sites together with the magnetization curve for $L=120 \times 120$. Comparing these results one can see that a magnetization plateau at $m^{sp}/m_s^{sp}=1/7$ is formed and that the region of its stability is practically independent of L .

Although we have considered the clusters of different classes (the 70×70 and 140×140 clusters are not dividable by 3 and the 120×120 cluster is not dividable by 7) the convergence of numerical results to $1/2$, $1/3$, $1/5$, and $1/7$ plateaus is apparent, what indicates that at least these plateaus persist in the thermodynamic limit. Performing the same numerical analysis on the 90×90 and 110×110 clusters we have found that the magnetization plateaus at $m^{sp}/m_s^{sp}=1/9$ ($L=90 \times 90$) and $m^{sp}/m_s^{sp}=1/11$ ($L=110 \times 110$) are also stable but their stability regions are very narrow ($\Delta h=10^{-3}$ for $m^{sp}/m_s^{sp}=1/9$ and $\Delta h=5 \times 10^{-4}$ for $m^{sp}/m_s^{sp}=1/11$).

The magnetization process of the electron subsystem is very similar to one described above for the spin subsystem but only in the limit $m^{sp}/m_s^{sp} \leq 0.5$ (see insets of Figs. 3–5). Indeed, we have found that for $m^{sp}/m_s^{sp} \leq 0.5$ the magnetization curves of electron and spin subsystems fully coincide for the strong coupling ($J_z=4$) between electron and spin subsystems, and small deviations are observed only for the intermediate coupling ($J_z=2$). However, a different picture of magnetization processes of electron and spin subsystems is observed in the limit $m^{sp}/m_s^{sp} > 0.5$. In this limit the spin subsystem is already fully saturated while the magnetization of the electron subsystem changes continuously from $m^{el}/m_s^{el}=0.5$ to $m^{el}/m_s^{el}=1$.

Finally, let us briefly discuss two important questions concerning: (i) the stability of plateau phases with $m^{sp}/m_s^{sp} \neq 1/3$ in the limit of $t \rightarrow 0$ and (ii) the origin of the physical mechanism leading to the resulting spin stripe ordering described above. To answer the first question we have performed the exhaustive numerical study of the model at $t=0.1$ and $t=0.01$. We have found that already such small values of t stabilize the $1/2$ and $1/5$ plateaus but their stability regions are very narrow ($\Delta h < 10^{-4}$). Moreover, the strong

finite-size effects have been observed in the limit of $t \rightarrow 0$ (even on clusters with $L > 100 \times 100$ sites) and thus it is questionable whether these plateaus persist in the thermodynamic limit. The second question is more difficult. At present the physical mechanism leading to various spin superstructures is not understood satisfactorily even for the spin-one-half Falicov-Kimball model with the anisotropic Ising interaction,^{13,14} that is the subset of our model ($J=0, J'=0$). It is supposed¹⁴ that driving mechanism leading to various spin superstructures in this model should be the same as was found recently by Brydon and Gulacsi¹⁷ for the spinless Falicov-Kimball model (the competition between the forward scattering and backscattering of itinerant electrons) but the rigorous proof has not been done for the spin version till now. For our extended model the situation is further complicated by the presence of the Ising spin subsystem that has a tendency to form the antiferromagnetic spin ordering for small values of h , the ferrimagnetic stripe ordering for intermediate h , and the ferromagnetic ordering for large h . Obviously, this is the competition between these tendencies and ones of the spin-one-half Falicov-Kimball model with anisotropic interaction^{13,14} that are responsible for the resulting spin stripe ordering. However, it will be necessary to perform additional numerical studies of our extended model (including the calculations of various correlation functions for both itinerant and localized particles) to understand completely the physical mechanism leading to the observed stripe ordering.

In summary, we have presented an alternative model of stabilization the magnetization plateaus in rare-earth tetraborides based on the coexistence of spin and electron subsystems (coupled by the anisotropic spin-dependent interaction of the Ising type) in these materials. It was shown that the switching on of the spin-dependent interaction between the electron and spin subsystems and taking into account the electron hopping on the nearest and next-nearest lattice sites of the SSL leads to a stabilization of four relevant magnetization plateaus at $m^{sp}/m_s^{sp}=1/2$, $1/3$, $1/5$, and $1/7$ of the saturated spin magnetization. The ground states corresponding to these magnetization plateaus have the same structure consisting of parallel antiferromagnetic bands of width $w=1, 2, 4$, and 6 separated by ferromagnetic stripes. These results indicate that the electron subsystem and its interaction with the spin subsystem can play the crucial role in the correct description of magnetization processes in rare-earth tetraborides. In our future work we plan to generalize this simple model by including the long-range interactions (it was shown that such interactions suppress the stability of the $1/3$ phase¹⁸) and considering the Heisenberg spins instead of the Ising ones.

ACKNOWLEDGMENTS

This work was supported by Slovak Grant Agency VEGA under Grant No. 2/0175/10, Slovak Research and Development Agency (APVV) under Grant No. VVCE-0058-07, and by the ERDF EU grant, under Contract No. ITMS26220120005. H.C. acknowledges support of Stefan Schwartz Foundation.

- ¹B. Sriram Shastry and B. Sutherland, *Physica B & C* **108**, 1069 (1981).
- ²H. Kageyama, K. Yoshimura, R. Stern, N. V. Mushnikov, K. Onizuka, M. Kato, K. Kosuge, C. P. Slichter, T. Goto, and Y. Ueda, *Phys. Rev. Lett.* **82**, 3168 (1999); K. Kodama, M. Takigawa, M. Horvatic, C. Berthier, H. Kageyama, Y. Ueda, S. Miyahara, F. Becca, and F. Mila, *Science* **298**, 395 (2002).
- ³S. Sebastian, N. Harrison, P. Sengupta, C. Batista, S. Francoual, E. Palm, T. Murphy, N. Marcano, H. Dabkowska, and B. Gaulin, [arXiv:0707.2075](https://arxiv.org/abs/0707.2075) (unpublished).
- ⁴J. Dorier, K. P. Schmidt, and F. Mila, *Phys. Rev. Lett.* **101**, 250402 (2008); A. Abendschein and S. Capponi, *ibid.* **101**, 227201 (2008).
- ⁵K. Siemensmeyer, E. Wulf, H.-J. Mikeska, K. Flachbart, S. Gabáni, S. Mat'áš, P. Priputen, A. Efdokimova, and N. Shitsevalova, *Phys. Rev. Lett.* **101**, 177201 (2008).
- ⁶Z. Y. Meng and S. Wessel, *Phys. Rev. B* **78**, 224416 (2008).
- ⁷M. C. Chang and M. F. Yang, *Phys. Rev. B* **79**, 104411 (2009).
- ⁸F. Liu and S. Sachdev, [arXiv:0904.3018](https://arxiv.org/abs/0904.3018) (unpublished).
- ⁹S. Michimura, A. Shigekawa, F. Iga, M. Sera, T. Takabatake, K. Ohoyama, and Y. Okabe, *Physica B* **378-380**, 596 (2006).
- ¹⁰S. Mat'áš, K. Siemensmeyer, E. Wheeler, E. Wulf, R. Beyer, Th. Hermannsdorfer, O. Ignatchik, M. Uhlarz, K. Flachbart, S. Gabáni, P. Priputen, A. Efdokimova, and N. Shitsevalova, *J. Phys.: Conf. Ser.* **200**, 032041 (2010).
- ¹¹S. Yoshii, T. Yamamoto, M. Hagiwara, S. Michimura, A. Shigekawa, F. Iga, T. Takabatake, and K. Kindo, *Phys. Rev. Lett.* **101**, 087202 (2008).
- ¹²R. Lemański, *Phys. Rev. B* **71**, 035107 (2005).
- ¹³P. Farkašovský and H. Čenčariková, *Eur. Phys. J. B* **47**, 517 (2005).
- ¹⁴R. Lemański and J. Wrzodak, *Phys. Rev. B* **78**, 085118 (2008).
- ¹⁵P. Farkašovský, *Eur. Phys. J. B* **20**, 209 (2001).
- ¹⁶H. Čenčariková and P. Farkašovský, *Int. J. Mod. Phys. B* **18**, 357 (2004).
- ¹⁷P. M. R. Brydon and M. Gulacsi, *Phys. Rev. B* **73**, 235120 (2006).
- ¹⁸T. Suzuki, Y. Tomita, and N. Kawashima, *Phys. Rev. B* **80**, 180405(R) (2009).